

**MASSACHUSETTS INSTITUTE OF TECHNOLOGY
HAYSTACK OBSERVATORY
WESTFORD, MASSACHUSETTS 01886**

August 4, 2020

Telephone: 617-715-5517

Fax: 617-715-0590

To: IVS VGOS Correlation Groups

From: J. Barrett, R. Cappallo, B. Corey, P. Elosegui, D. Mondal, A. Niell, C. Rusczyk, and M. Titus

Subject: VGOS intensive VI9290 follow-up test

1 Introduction

During the initial examination of the correlation and data processing of the VGOS intensive session VI9290 by multiple correlation centers, some differences were discovered in the results provided by each center at several stages of the process¹. One particularly egregious issue was the existence of a handful of scans which exhibited very large differences ($> 10^4$ ps) in the total multi-band delay (τ_{MBD}). A cursory examination of these scans led to the conclusion that this was due to corruption of the raw data during the conversion of multi-threaded VDIF data to single-threaded VDIF². To test this hypothesis, the VDIF data as processed by the Haystack correlator (gathered and de-threaded) was sent for re-processing at Vienna (who graciously volunteered to re-execute the original test) with the additional step of verifying the integrity of the data via a checksum. Beyond the handful of scans which exhibited very large total multi-band delay differences it was also noted most of the other scans also exhibited differences in the τ_{MBD} , albeit at much much smaller level. This was largely due to the fact that the correlator clock model (as well as the manner in which the pseudo-Stokes-I fourfit control file was constructed) diverged between the correlation centers. Therefore, in order to eliminate these smaller differences, an update (to HOPS 3.21-r2936) was applied to the post-processing scripts used for the generation of the fourfit control so as to ensure any a priori additive phase calibration (pc_phases) are applied to all stations (including the network phase reference station). Furthermore, Vienna was also instructed to use Haystack's clock model for correlation so that any other possible causes for the differences in the results might be detected.

Along with Vienna, two additional correlation centers (Tsukuba and Onsala) requested data to participate in the blind-test exercise of VI9290. At the time, the follow-up to the initial test was still in progress so while both Tsukuba and Onsala performed this test with the updated post-processing software (HOPS 3.21-r2936) they each developed their own clock models for the correlation. As such their results are similar to the other correlation centers which participated in the original test (see VGOS memo #51), and as expected, were not entirely identical with Haystack's results.

2 Results

2.1 Onsala and Tsukuba

Onsala obtained the data for this exercise from Bonn's copy of the e-transferred data (vmux'ed by Bonn from the gathered station data as part of the original blind-test). As such a few of the scans which they correlated suffered from the same data corruption seen in the original test. They also derived their own clock model for the correlation. Tsukuba obtained a copy of the (pre-gathered and de-threaded data) from Haystack, and also derived their own clock model. A comparison of the EOPs used are shown in figures 1 to 3 and clock model parameters are listed in table 1. During post-processing both Onsala and Tsukuba used the initial control file provided by

¹See VGOS memo #51.

²This conversion is normally done by the stations before e-transfer but was omitted in the case of VI9290, and as such the correlation centers had to perform the conversion.

Haystack (containing the a priori pc_phases) and using the updated software (HOPS 3.21-r2936) were each able to generate a production pseudo-Stokes-I control file which were quite close to Haystack's. Figures 4 through 7 compare the pc_phases for each station specified in the production fourfit control file by each correlation center and show that the a priori pc_phases were carried over and applied to the phase reference station (Kokee, H) (figures 4, 5), while the pc_phases generated for Wettzell (V) (figures 6, 7) are the same between the three correlation centers to within roughly 5 degrees. Table 2 compares the Y-X phase and delay offsets generated by each correlator, and shows they are consistent to within the estimated error.

To further compare the results of Onsala and Tsukuba, the following quantities were examined with respect to Haystack:

1. The SNR of each scan-baseline.
2. The residual multi-band delay of each scan-baseline as function of time.
3. The differential total electron content (dTEC) of each scan-baseline.
4. The total multi-band delay of each scan-baseline.
5. The proxy cable-calibration delays.

The difference of these quantities with respect to Haystack are shown for Onsala and Tsukuba in figures 8 and 9 respectively. It should be noted that out of the full data-set several scans were flagged as being outliers for each correlator. Onsala's data-set contains three scans which were flagged as having unusually large differences in the total multi-band delay ($\Delta\tau_{MBD} > 100\text{ps}$ – 290-1906, 290-1912, 290-1927), while in Tsukuba's results the scans 290-1849, 290-1906 and 290-1927 were flagged. Unsurprisingly, most of these scans (290-1906, 290-1912, and 290-1927) were also flagged as outliers in the original blind-test comparison. However, while the large differences in τ_{MBD} exhibited in Onsala's results could perhaps be explained solely by data corruption (as they used Bonn's data), Tsukuba used data which was gathered and vmux'ed at Haystack, therefore (short of the possibility of coincidental corruption of some of the same scans during e-transfer) it is unlikely these differences in τ_{MBD} were entirely introduced by data corruption alone.

In addition, the proxy cable-calibration delays derived by Onsala and Tsukuba were compared to Haystack's values and are shown in figures 10, and 11 for Kokee and Wettzell respectively. The differences are relatively small (as the band-polarizations chosen during averaging were the same as Haystack). There were however a handful of scans where there was a slight jump in the differences, but these were all less than 1 picosecond.

2.2 Vienna

The re-processing exercise performed by Vienna went through several stages as various difficulties were overcome. Vienna's results were also compared with Haystack by examining the quantities listed above.

Figure 16 shows the data-set created from Vienna's first re-correlation of the data during the follow-up test as compared to Haystack. One immediate conclusion drawn from this initial comparison of the data was that there was no longer any scans with exceedingly large ($> 20\text{ ps}$) differences in the total multi-band delay. This appears to lend some credence to the hypothesis that at least some of the differences seen in particular scans (e.g. 290-1901, 290-1927, etc.) which exhibited large differences in τ_{MBD} during the original study may have been due to the corruption of the raw data during the vmux-ing step or during the e-transfer of the data. Unfortunately, this was not the only cause of differences in τ_{MBD} and it was realized soon after that in the first-pass of the follow-up study Vienna's copy of the HOPS post-processing software had not yet been updated to (HOPS 3.21-r2936) to incorporate the updates made after the first blind-test. The use of the old software caused the control file generation script to drop any a priori pc_phases (additive phase cal. corrections) applied to the X-polarization of the network reference station in the initial control file and subsequently set them to zero in the final control file.

This problem is clearly shown in figure 12, as the pc_phases specified in the fourfit control-file provided by Vienna that are applied to the X-polarization of Kokee are all set to zero (labeled as 'vienna'). Vienna's data were re-processed locally at Haystack using the updated post-processing software, and the resulting pc_phases are shown

in the same figure (12) labeled as 'vienna2'. In this re-processing of the their data (using the corrected software) the `pc_phases` for Kokee X-polarization matched those found by the Haystack. Figure 17 compares Vienna's results to Haystack's data-set after this second post-processing pass, from which it is evident that that there were still some discrepancies in the data. Chief among these was a large offset in the residual multi-band delay. This was due to a difference in the clock models used by Vienna and Haystack. This difference was somewhat puzzling at first, since by design the data were re-correlated with the same clock model, station positions, and EOPs as Haystack. However, while care had been take to ensure that station positions and EOPs were identical, it was found that that clock model epoch was different (Haystack's being 18.5 hours later than from Vienna's). This was due to an accidental omission of this information from VGOS memo #51, and it caused the large offset (~ 3270 ps) in the residual multi-band delay differences between the two correlators. This difference in the clock models between the two correlators also had some small knock-on effect in the post-processing and caused the Y-X delay offset computed for K2 by Vienna to be less than Haystack's value by about 2 ps, this difference is visible in figure 17e where an offset of about -1.8 ps is visible in the total multi-band delay differences.

Once the clock model epoch was corrected so that the clock model's of both correlators matched, Vienna re-correlated the data and obtained results which matched Haystack's nearly exactly. Figure 18 shows the differences in the results between Haystack and Vienna's final correlation, from which it can be seen that the total multi-band delay values are are nearly identical.

The final consideration in the comparison of Vienna's results with Haystack were the derived values of the proxy-cable delay. As expected, for this test the results were essentially entirely consistent between Haystack and Vienna. This simply due to the fact that in the follow-up test the selected band-polarizations chosen to be averaged together were identical.

3 Conclusion

Osnala and Tsukuba completed the VI9290 blind test in a manner consistent with the other correlation centers and obtained similar results. Vienna executed a follow-up test to determine if the conclusions of the initial blind-test comparison were valid and addressed the differences seen between the results of each correlation center. This was mostly successful, as the largest differences in the data were eliminated by:

1. Re-transmitting the data to fix corrupted files.
2. Correlating with the exactly same station positions, EOPs, and clock model.
3. Re-running the post-processing on the correlated data with an updated version of the HOPS software to fix missing a priori `pc_phases` applied to the network reference station.
4. Ensuring that proxy-cable delay files were generated using the same choice of band-polarizations.

While this test was successful, it should be noted that perfect repeatability/consistency between each correlation center remains somewhat challenging. Overcoming these differences will likely need the specification of a consistent procedure to be used when constructing the correlator clock model. Furthermore, the use of a priori additive phase-cal corrections (`pc_phases`) are needed when generating the production pseudo-Stokes-I fourfit control file for each session, so some mechanism for tracking the value of these `pc_phases` between correlator centers should probably be established. In addition, the band-polarization choice which needs to be made when generating the proxy cable-calibration files should be done via some automatic means in order to make this decision less subjective. Work on automating this choice is in progress.

Quantity	MIT	Onsala	Tsukuba
Model validity start	2019y290d00h00m	2019y290d18h30m02s	2019y290d00h00m
Epoch	2019y290d18h30m	2019y290d18h30m02s	2019y290d18h30m
K2 offset (μs)	9.163	9.130	8.660
Ws offset (μs)	0.524	0.416	0.020
Net offset (K2-Ws) (μs)	8.639	8.714	8.46
Relative net offset w.r.t MIT (μs)	–	0.075	-0.179
K2 rate (ps/s)	-0.422	-1.562	-1.189
Ws rate (ps/s)	-0.002	-0.274	0.081
Net rate (K2-Ws) (ps/s)	-0.420	-1.288	-1.27
Relative net rate w.r.t MIT (ps/s)	–	-0.868	-0.707

Table 1: Comparison of the correlator clock models for Haystack, Onsala and Tsukuba.

Quantity	MIT	Tsukuba	Onsala
K2 Y-X delay offset (ns)	0.141 ± 0.002	0.137 ± 0.003	0.138 ± 0.003
Ws Y-X delay offset (ns)	-0.057 ± 0.003	-0.06 ± 0.002	-0.059 ± 0.003
K2 Y-X phase offset (deg)	-44.2 ± 3.7	-45.1 ± 3.2	-46.5 ± 3.0
Ws Y-X phase offset (deg)	-132.8 ± 4.0	-133.9 ± 5.7	-139.0 ± 3.1

Table 2: Comparison of Y-X polarization delay and phase offsets generated for each station (K2 and Ws) by Tsukuba and Onsala.

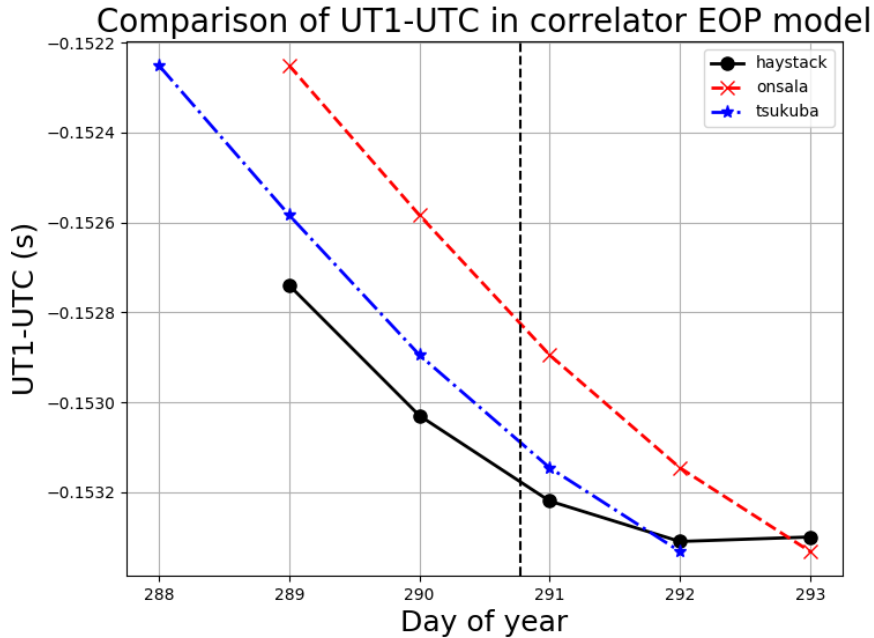


Figure 1: Value of UT1-UTC from EOP models of Onsala and Tsukuba as compared to Haystack. The vertical black dashed line marks the start of VI9290.

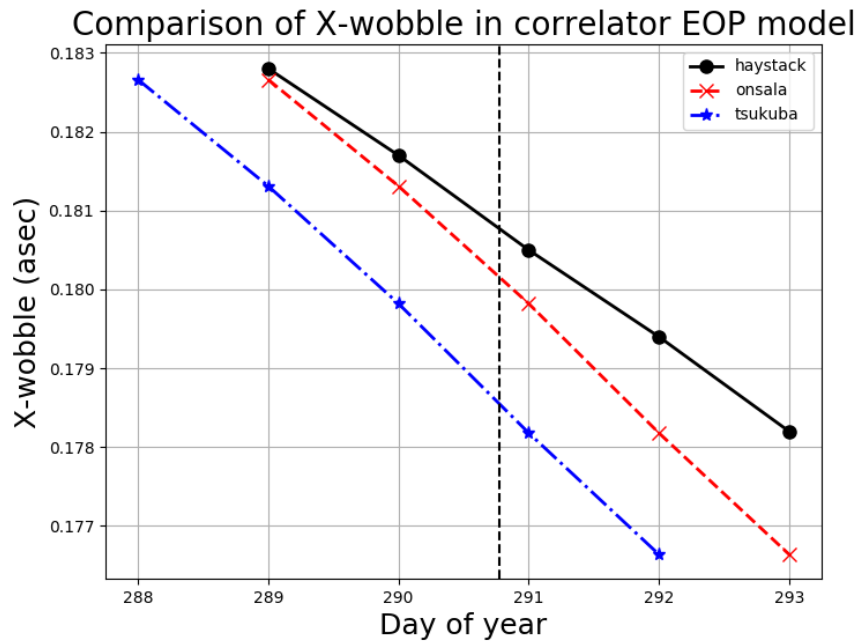


Figure 2: Value of the X-wobble parameter from EOP models of Onsala and Tsukuba as compared to Haystack. The vertical black dashed line marks the start of VI9290.

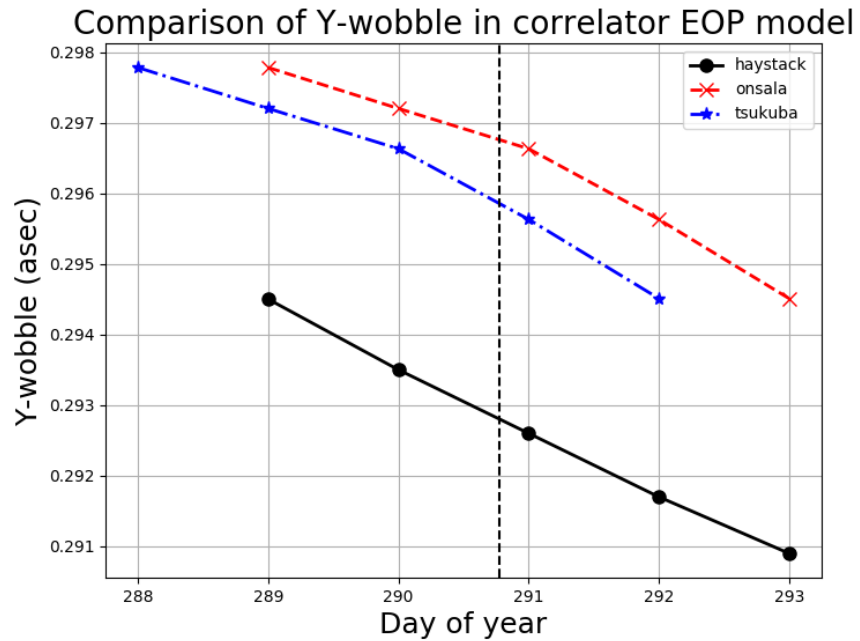


Figure 3: Value of the Y-wobble parameter from EOP models of Onsala and Tsukuba as compared to Haystack. The vertical black dashed line marks the start of VI9290.

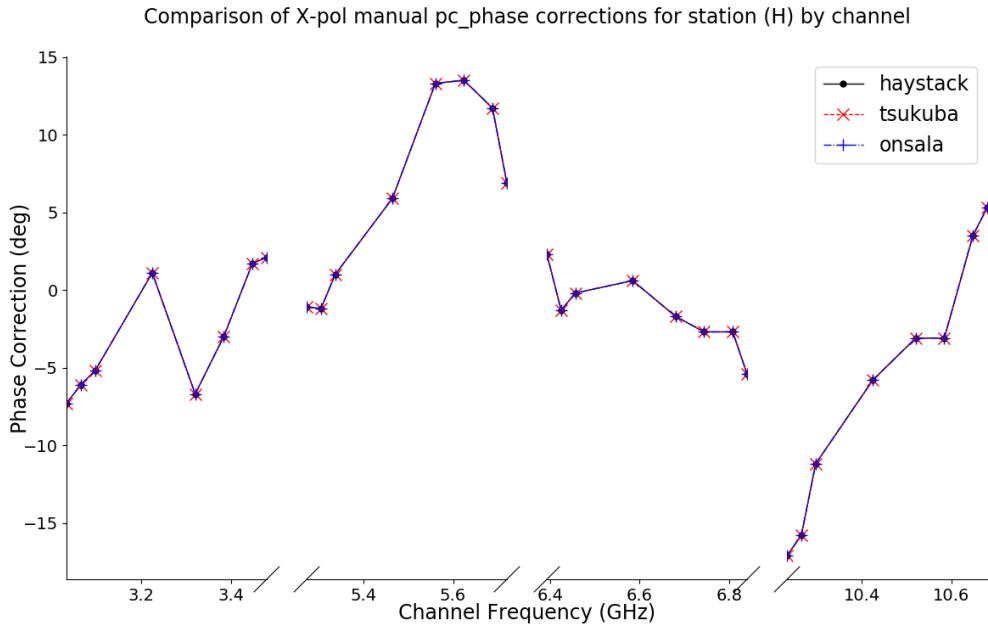


Figure 4: Kokee X-polarization pc_phases for Onsala and Tsukuba as compared to Haystack.

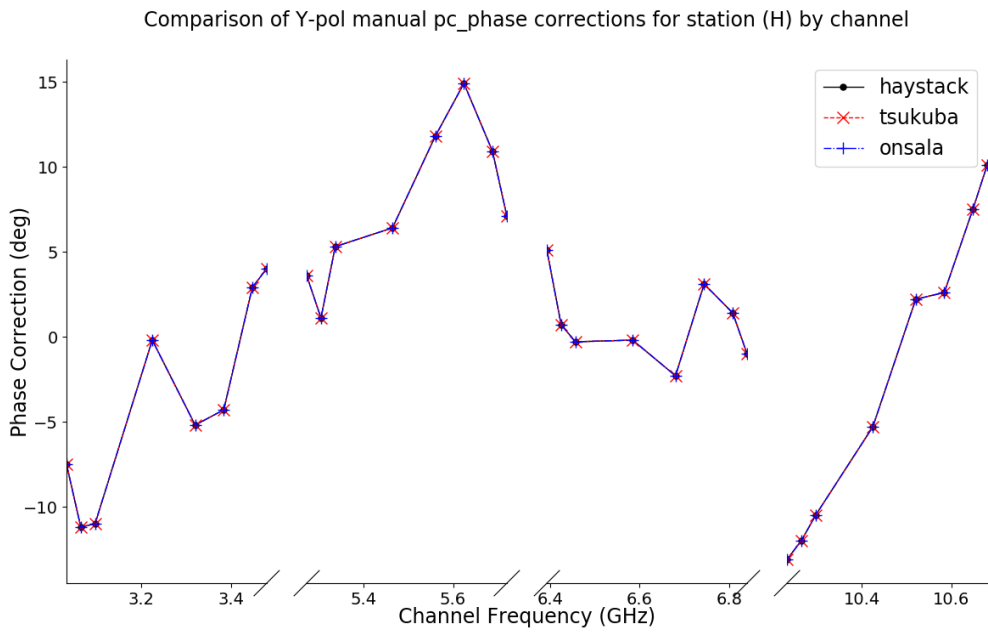


Figure 5: Kokee Y-polarization pc_phases for Onsala and Tsukuba as compared to Haystack.

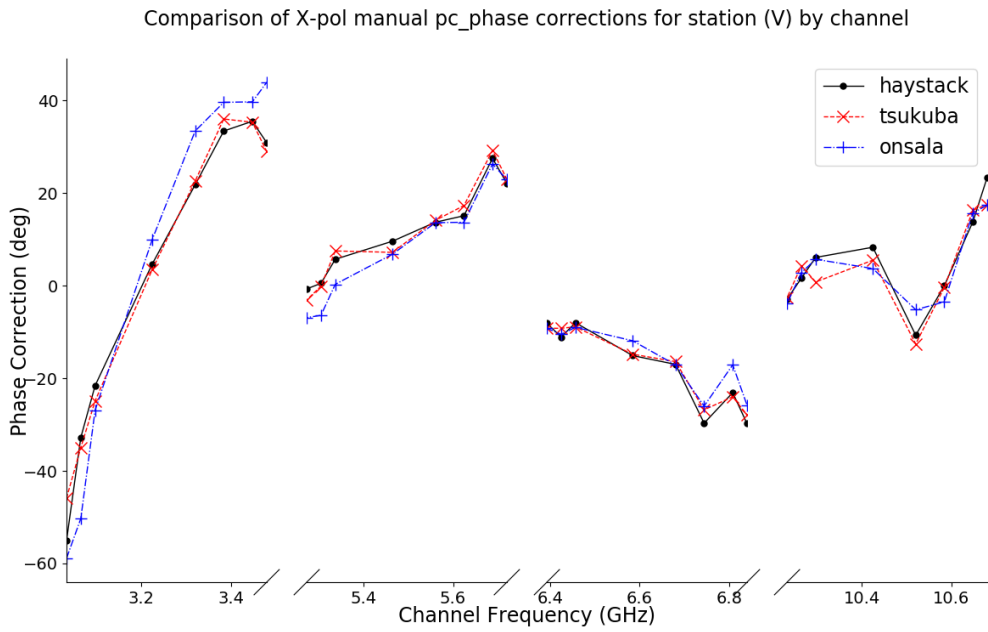


Figure 6: Wettzell X-polarization pc_phases for Onsala and Tsukuba as compared to Haystack.

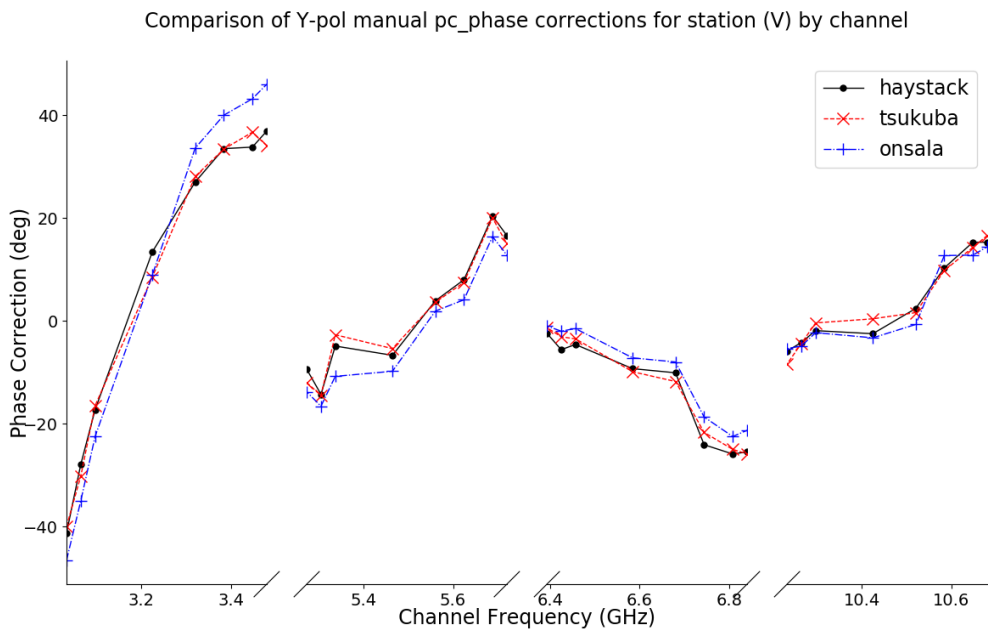
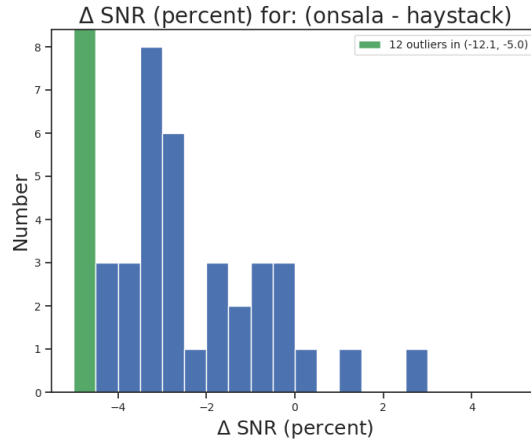
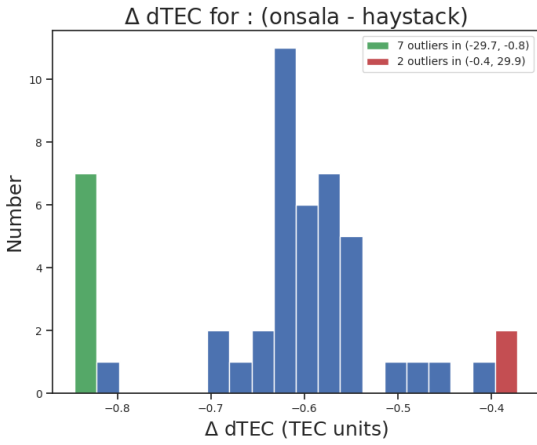


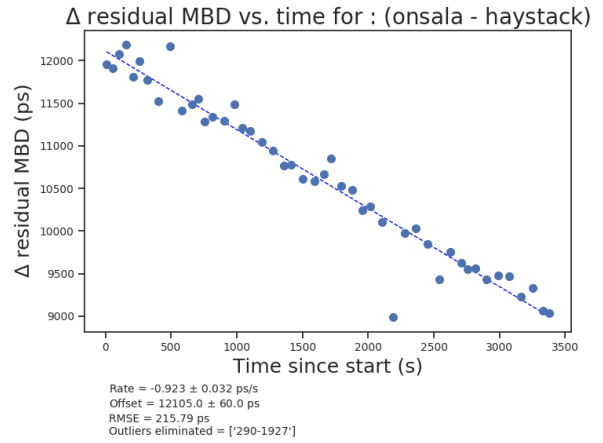
Figure 7: Wettzell Y-polarization pc_phases for Onsala and Tsukuba as compared to Haystack.



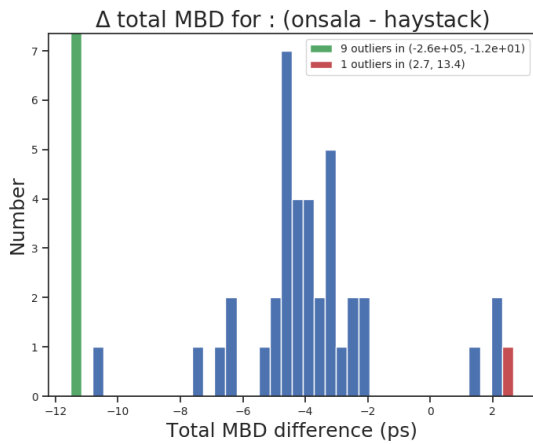
(a) Distribution of the difference in scan SNR



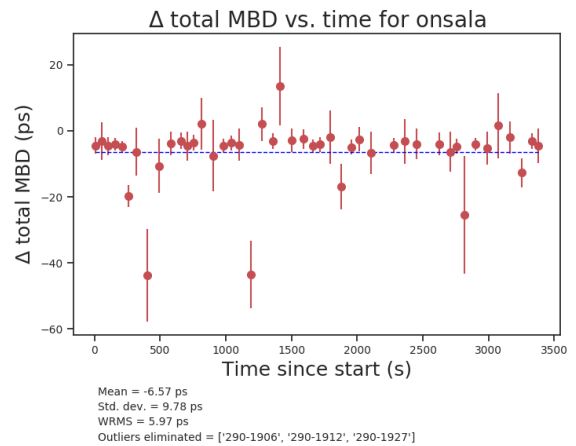
(b) Distribution of the difference in the scan dTEC



(c) Difference in the residual multi-band delay as a function of time since start.

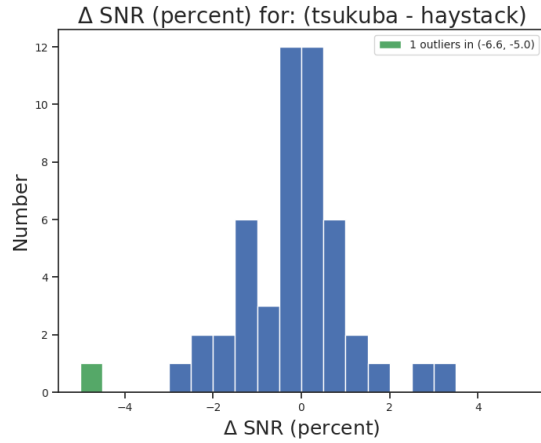


(d) Distribution of the difference in the total multi-band delay

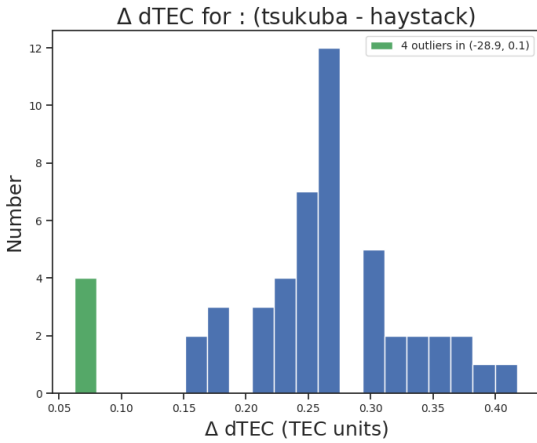


(e) Difference in the total multi-band delay as a function of time since start

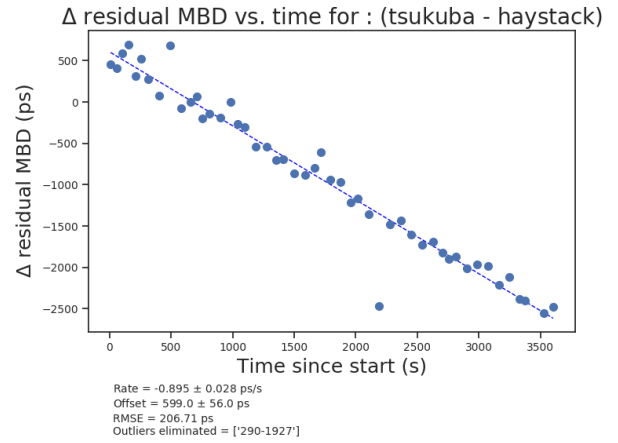
Figure 8: Comparison of Onsala data with Haystack for VI9290.



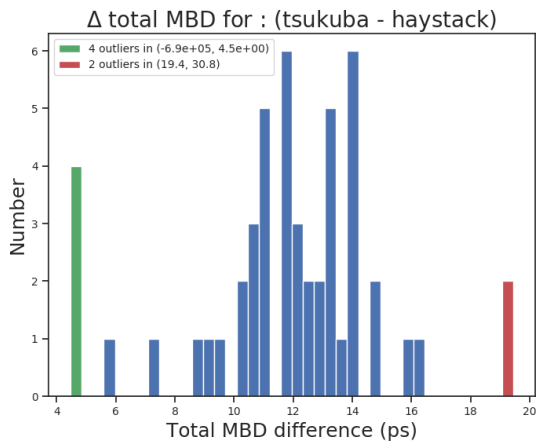
(a) Distribution of the difference in scan SNR



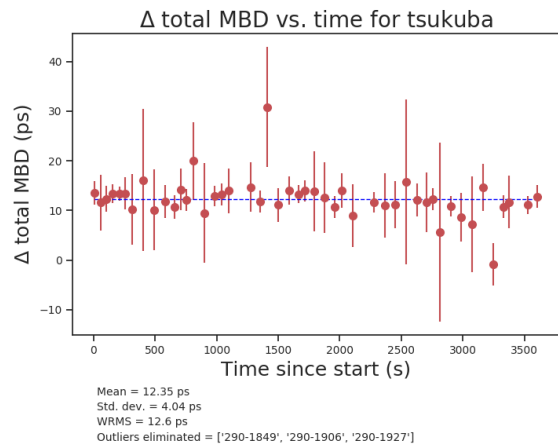
(b) Distribution of the difference in the scan dTEC



(c) Difference in the residual multi-band delay as a function of time since start.



(d) Distribution of the difference in the total multi-band delay



(e) Difference in the total multi-band delay as a function of time since start

Figure 9: Comparison of Tsukuba data with Haystack for VI9290.

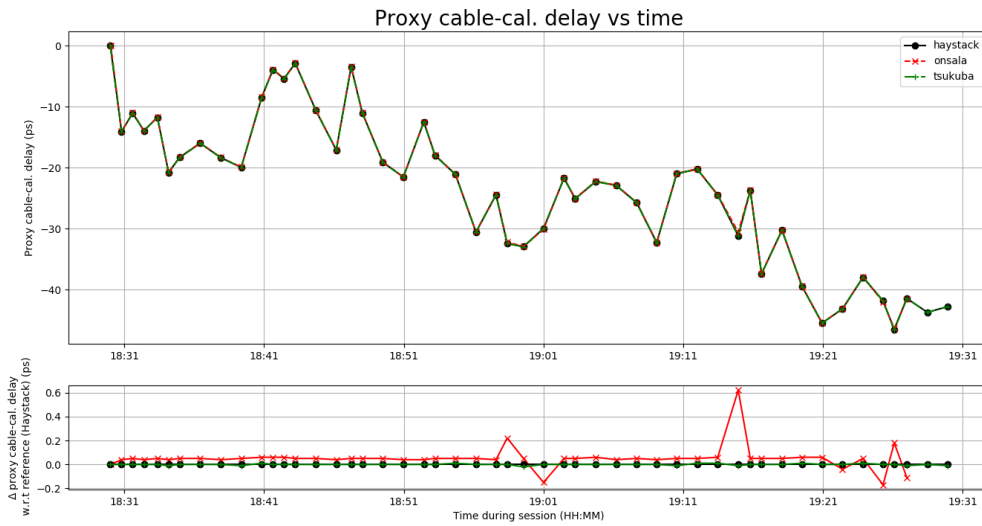


Figure 10: Comparison of proxy cable delay derived for Kokee by Onsala and Tsukuba.

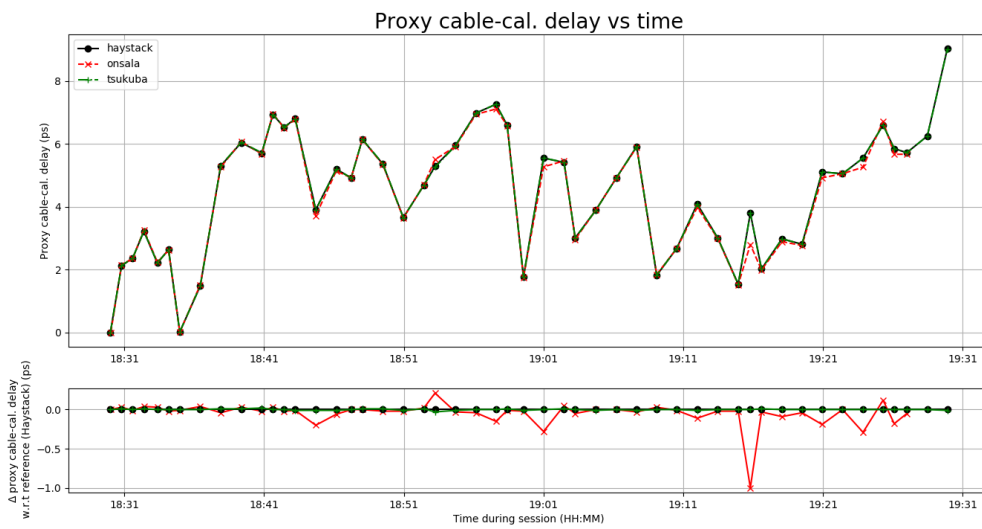


Figure 11: Comparison of proxy cable delay derived for Wettzell by Onsala and Tsukuba.

Quantity	MIT	Vienna
Model validity start	2019y290d00h00m	2019y290d00h00m
Rate Epoch	2019y290d18h30m	2019y290d00h00m
K2 offset (μs)	9.163	9.163
Ws offset (μs)	0.524	0.524
Net offset (K2-Ws) (μs)	8.639	8.639
Relative net offset w.r.t MIT (μs)	–	0.0
K2 rate (ps/s)	-0.422	-0.422
Ws rate (ps/s)	-0.002	-0.002
Net rate (K2-Ws) (ps/s)	-0.420	-0.420
Relative net rate w.r.t MIT (ps/s)	–	0.0

Table 3: Comparison of the correlator clock models for Haystack and Vienna (during first pass of the follow-up test). During the second pass of the follow-up test Vienna correlated the data with the exact same clock model as Haystack. Note that difference between the two models during the first pass is highlighted in red. The station positions and EOPs used by Vienna were the same as Haystacks and are not shown here.

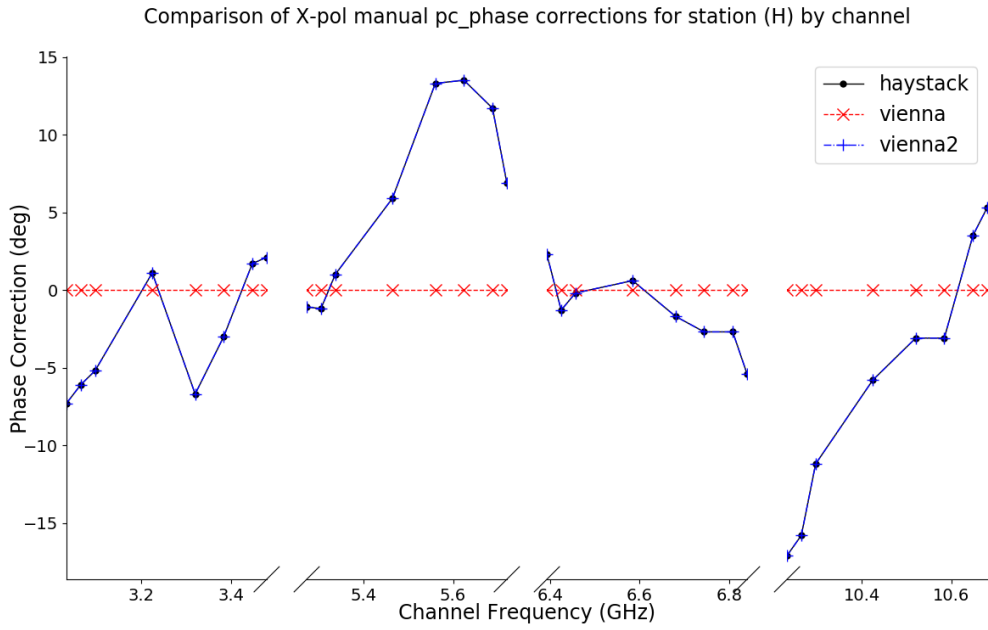


Figure 12: Kokee X-polarization pc_phases derived by Vienna as compared to Haystack. In this plot the initial pc_phases found by Vienna during the first pass of the follow-up test are labeled 'vienna', while the pc_phases found by Vienna after correcting the clock model and post-processing software version are labeled 'vienna2'.

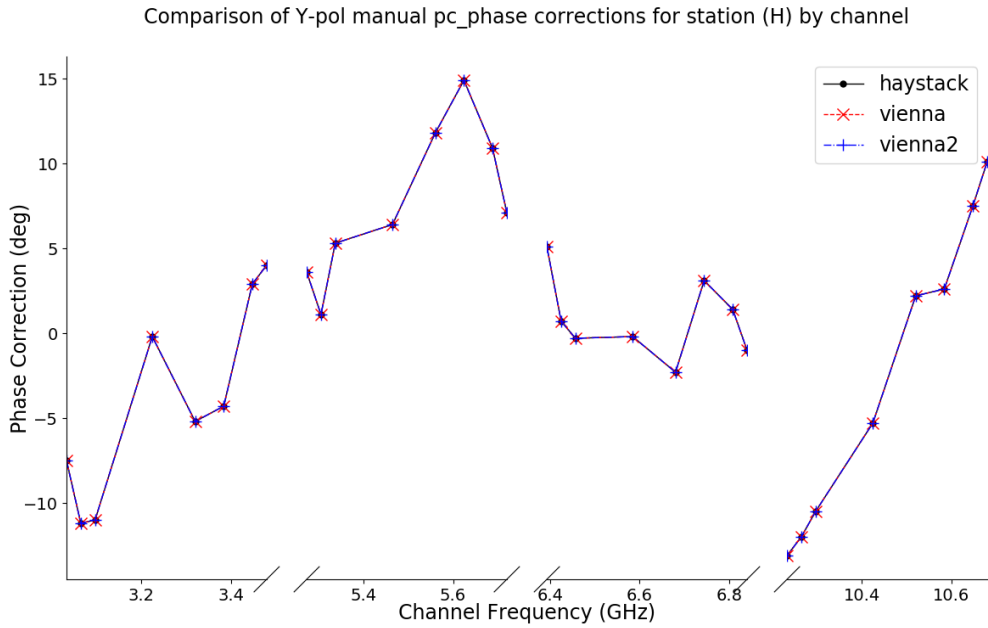


Figure 13: Kokee Y-polarization pc_phases derived by Vienna as compared to Haystack. In this plot the initial pc_phases found by Vienna during the first pass of the follow-up test are labeled 'vienna', while the pc_phases found by Vienna after correcting the clock model and post-processing software version are labeled 'vienna2'.

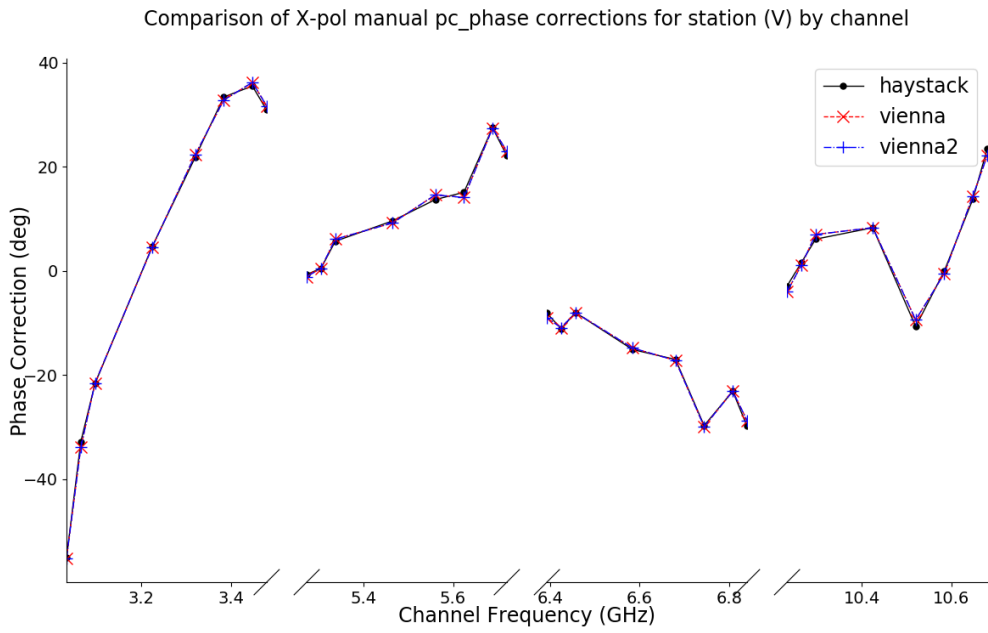


Figure 14: Wettzell X-polarization pc_phases derived by Vienna as compared to Haystack. In this plot the initial pc_phases found by Vienna during the first pass of the follow-up test are labeled 'vienna', while the pc_phases found by Vienna after correcting the clock model and post-processing software version are labeled 'vienna2'

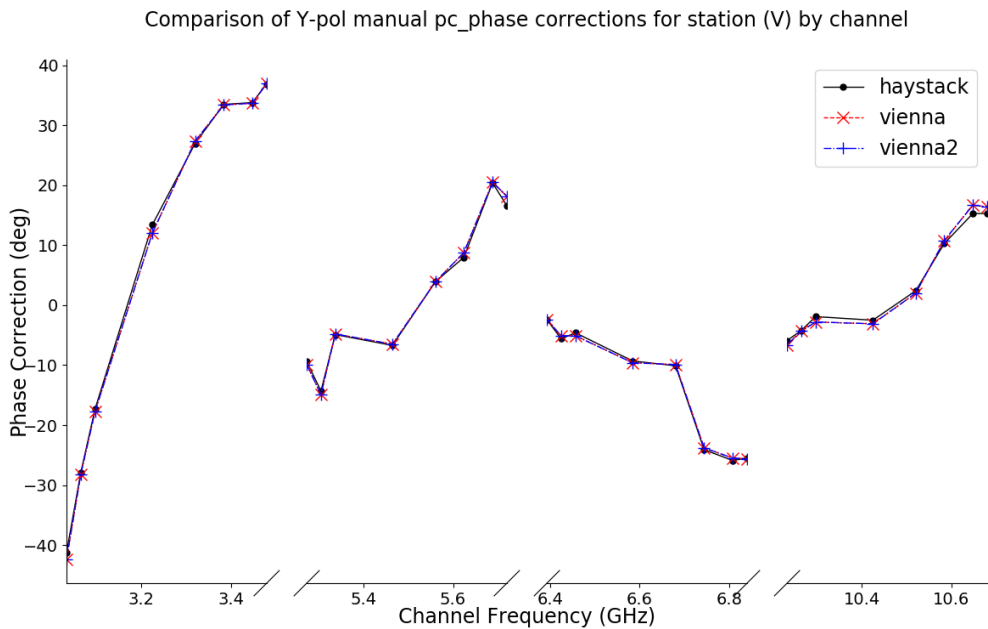
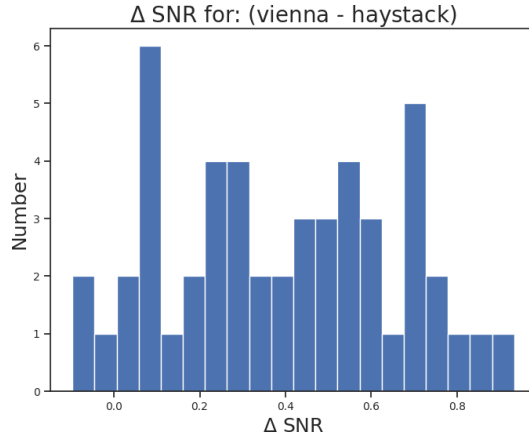
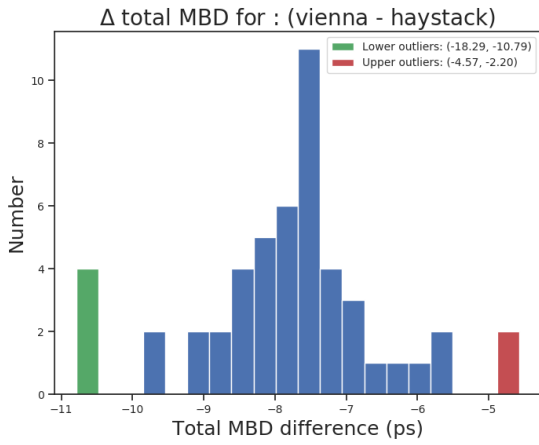


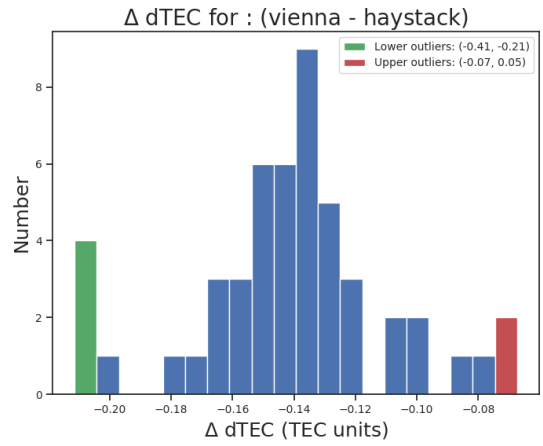
Figure 15: Wettzell Y-polarization pc_phases derived by Vienna as compared to Haystack. In this plot the initial pc_phases found by Vienna during the first pass of the follow-up test are labeled 'vienna', while the pc_phases found by Vienna after correcting the clock model and post-processing software version are labeled 'vienna2'



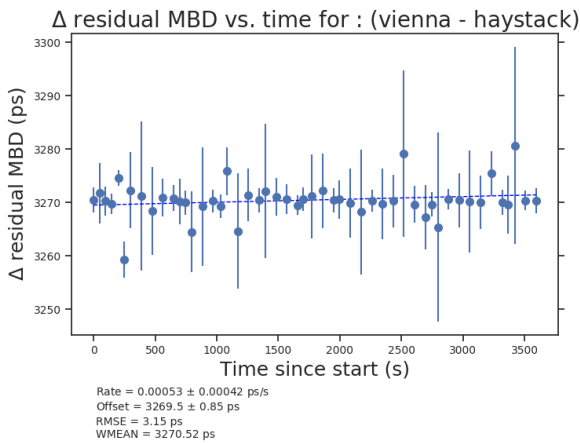
(a) Distribution of the difference in scan SNR



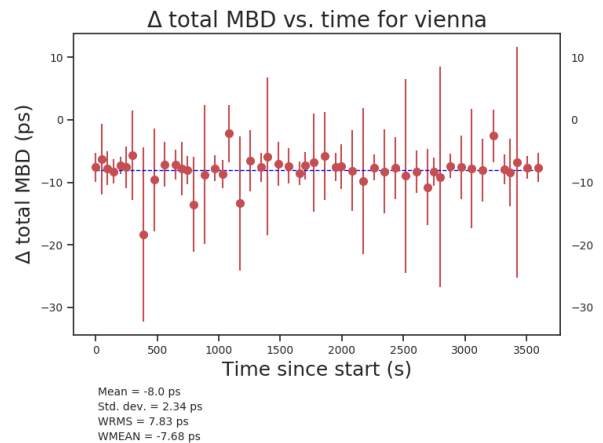
(b) Distribution of the difference in the total multi-band delay



(c) Distribution of the difference in the scan dTEC

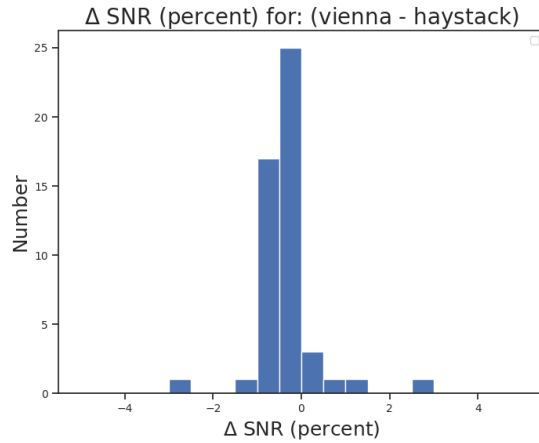


(d) Difference in the residual multi-band delay as a function of time since start.

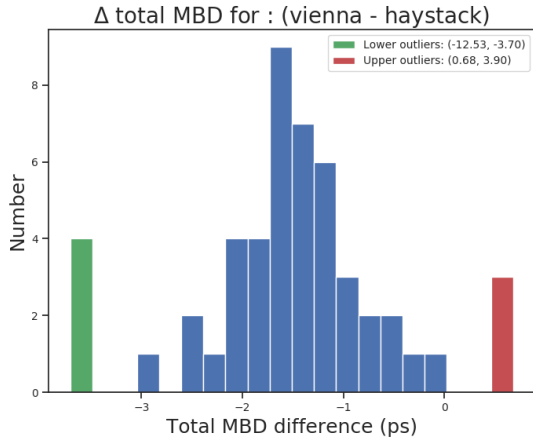


(e) Difference in the total multi-band delay as a function of time since start

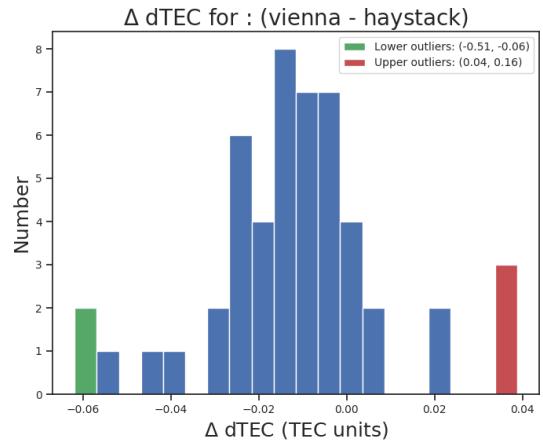
Figure 16: Comparison of Vienna data with Haystack for VI9290, during the first pass of the follow-up test. During this portion of the test Vienna used slightly different clock model, and the old post-processing software (HOPS 3.21).



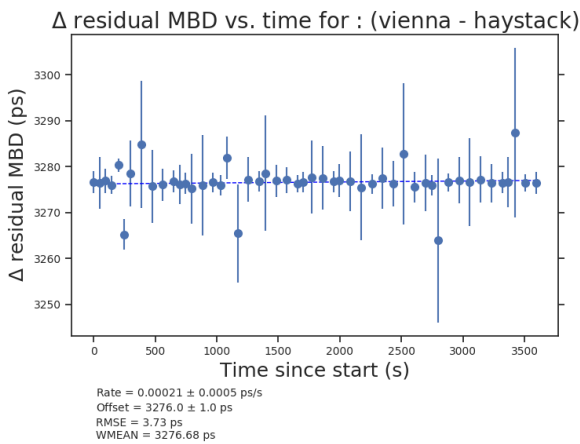
(a) Distribution of the difference in scan SNR



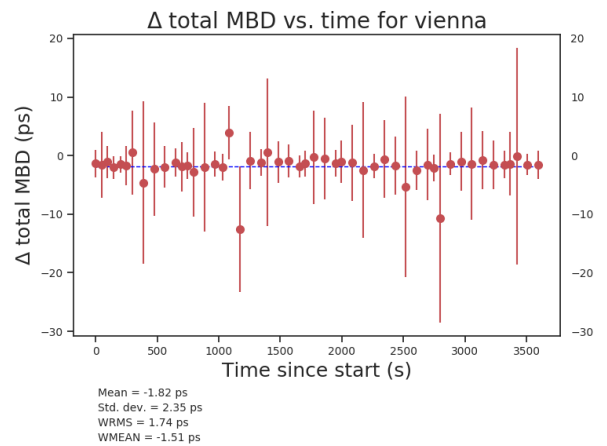
(b) Distribution of the difference in the total multi-band delay



(c) Distribution of the difference in the scan dTEC

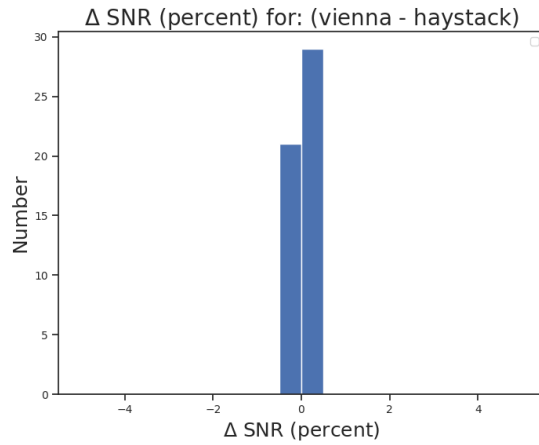


(d) Difference in the residual multi-band delay as a function of time since start.

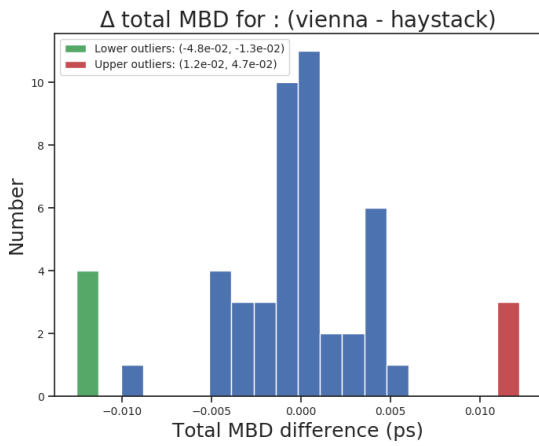


(e) Difference in the total multi-band delay as a function of time since start

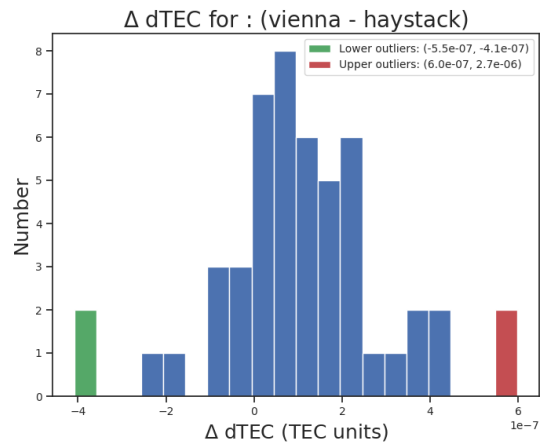
Figure 17: Comparison of Vienna data with Haystack for VI9290, during the second pass of the follow-up test. During this portion of the test Vienna ran the post-processing with the updated software (HOPS 3.21-r2936). However, the data had been correlated with a slightly different clock model (using a different epoch), this resulted in slightly different control file parameters (namely the Y-X phase/delay offsets) which are responsible for the -1.82 ps offset in figure 17e.



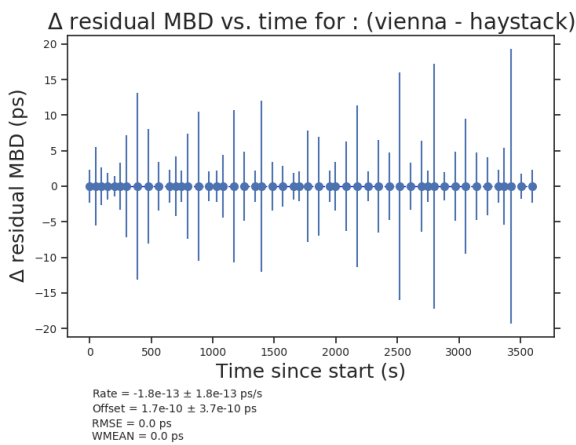
(a) Distribution of the difference in scan SNR



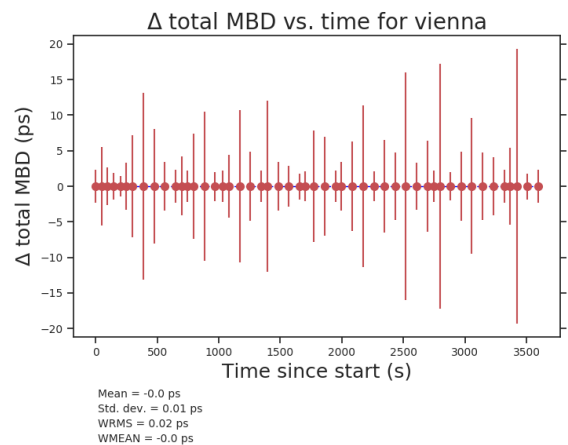
(b) Distribution of the difference in the total multi-band delay



(c) Distribution of the difference in the scan dTEC



(d) Difference in the residual multi-band delay as a function of time since start.



(e) Difference in the total multi-band delay as a function of time since start

Figure 18: Comparison of Vienna data with Haystack for VI9290, during the final pass of the follow-up test. During this portion of the test Vienna used exactly the same clock model and the updated post-processing software (HOPS 3.21-r2936). Note that the differences are now extremely small.

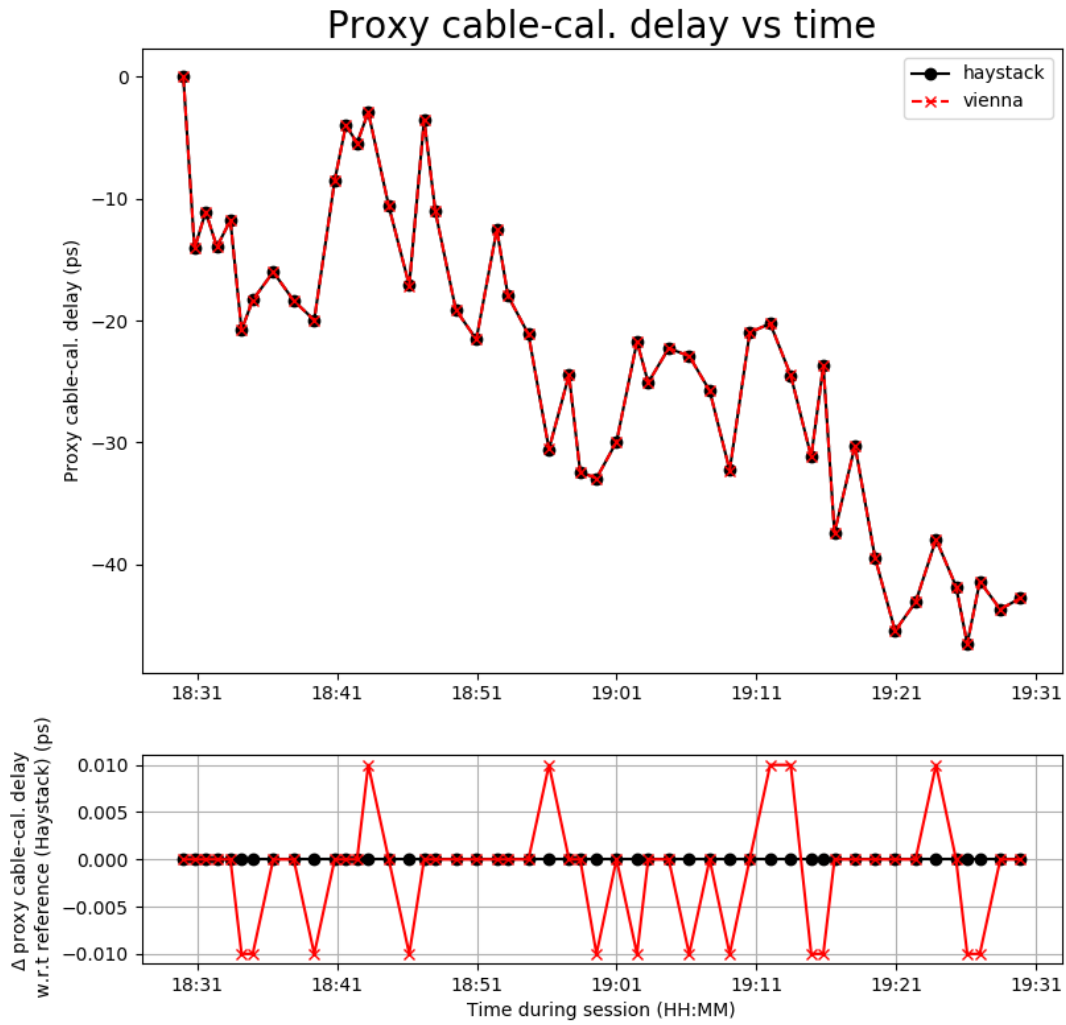


Figure 19: Comparison of proxy cable delay derived for Kokee by Vienna.

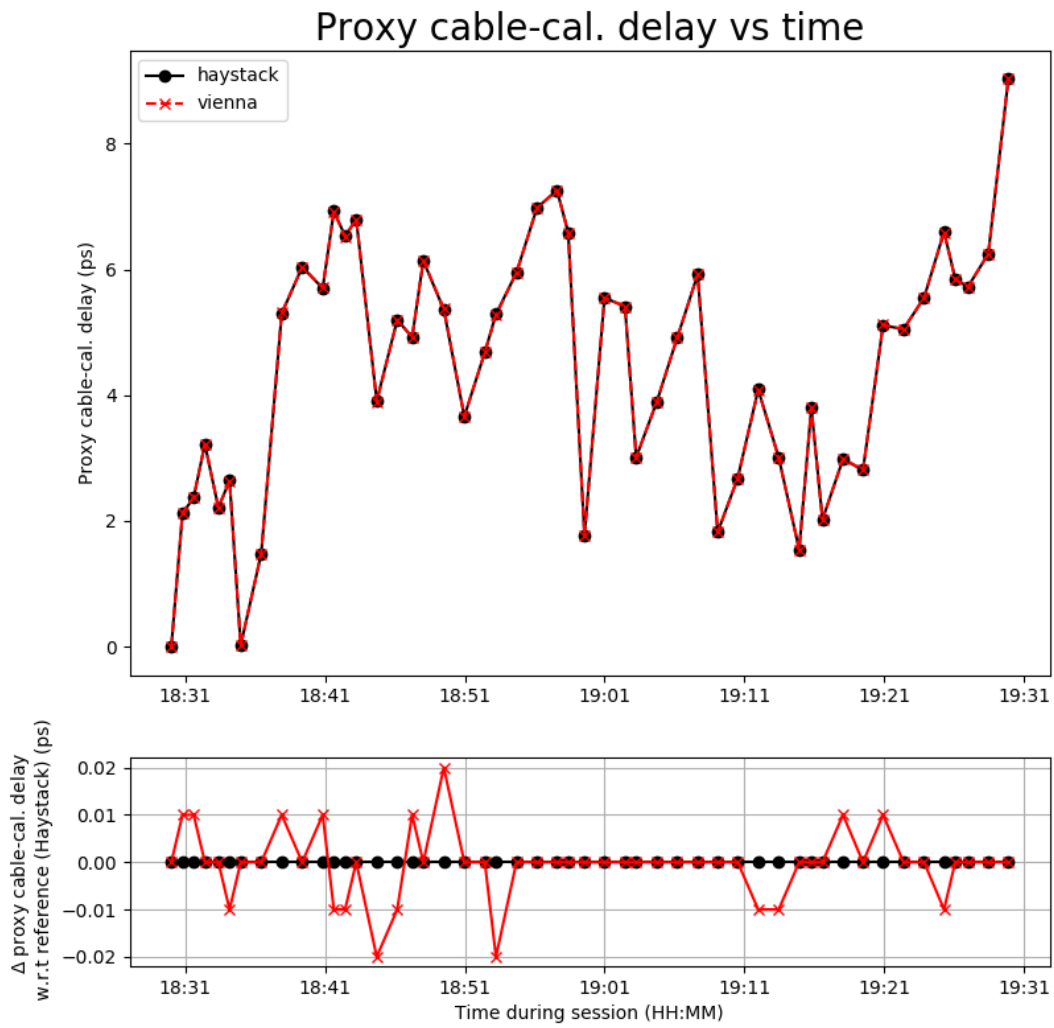


Figure 20: Comparison of proxy cable delay derived for Wetzell by Vienna.